Pharmacological evidence for the bone-autonomous contribution of the NFκB/β-catenin axis to breast cancer related osteolysis

Silvia Marino[a,b], Ryan T. Bishop[a], John G. Logan[b], Patrick Mollat[c] and Aymen I. Idris[a,b*]

Authors' Affiliations:

[a]Department of Oncology and Metabolism, University of Sheffield, Medical School, Beech Hill Road, Sheffield, S10 2RX, UK. [b]Bone and Cancer Group, Edinburgh Cancer Research Centre, MRC Institute of Genetics and Molecular Medicine, University of Edinburgh, EH4 2XR, UK. [c]Galapagos SASU, 102 Avenue Gaston Roussel, 93230 Romainville, France.

*Corresponding Authors: Department of Oncology and Metabolism, Medical School, Beech Hill Road, Sheffield, S10 2RX, UK. E-mail: aymen.idris@sheffield.ac.uk.

Running Title: Disruption of NFκB/B-catenin signalling reduces osteolysis.

Abbreviations: PTN, Parthenolide; NFκB, nuclear factor kappa-B; RANK, receptor activator of NFκB; RANKL, RANK ligand; TNFα, tumour necrosis factor alpha; IL1β, interleukin 1 beta; CD40L, Cluster of differentiation 40 ligand; TRAF, receptor-associated factor; IKK, IκB kinase; TGFβ, transforming growth factor beta; Runx2, runt related transcription factor 2; M-CSF, mouse macrophage colony stimulating factor; DMSO, Dimethyl sulfoxide; microCT, micro–computed tomography; TRAcP, tartrate-resistant acid phosphatase; Alk Phos, alkaline phosphatase; ALZ, alizarin red; BM, bone marrow; ANOVA, analysis of variance; SD, standard deviation.

Abstract

The NFκB signaling pathway is implicated in breast cancer and bone metastasis. However, the bone-autonomous contribution of NFκB to breast cancer-induced osteolysis is poorly understood. Here, we report that pretreatment of osteoblasts with the sesquiterpene lactone Parthenolide (PTN), a verified NFκB inhibitor, prior to exposure to conditioned medium from human and mouse breast cancer cell lines enhanced osteoblast differentiation and reduced osteoblast ability to stimulate osteoclastogenesis. PTN prevented breast cancer-induced osteoclast formation and reduced the ability of breast cancer cells to prolong osteoclast survival and to inhibit osteoclast apoptosis. *In vivo*, administration of PTN in immuno-competent mice reduced osteolytic bone loss and skeletal tumour growth following injection of the syngeneic 4T1-BT1 cells and reduced local osteolysis caused by conditioned medium from human and mouse osteotropic breast cancer cell lines. Mechanistic studies revealed that NFκB inhibition by PTN in osteoblasts and osteoclasts was accompanied by a significant increase in β-catenin activation and expression. Collectively, these results raise the possibility that combined targeting of NFκB and β-catenin signalling in the tumour microenvironment may be of value in the treatment of breast cancer related osteolysis.

Keywords: NFκB; β-catenin; breast cancer; osteolysis; bone.

Highlights

- Osteotropic human and mouse breast cancer cells are sensitive to NFκB inhibition.
- NFκB inhibition reduces osteoclast formation and osteoblast inhibition by breast cancer cells.
- The NFκB/β-catenin axis contributes to breast cancer-induced bone cell activity.
- Combined targeting of NFκB and β-catenin has potential efficacy in breast cancer osteolysis.

1. Introduction

Skeletal related events are a common cause of morbidity in patients diagnosed with secondary breast cancer in bone [1-3]. Bone metastases related to advanced breast cancer are osteolytic, and are caused by stimulation of osteoclast formation and bone resorption by breast cancer cells and/or their derived factors in the skeleton [3, 4]. A number of breast cancer- and bone-derived factors including receptor activator of nuclear factor kappa-B (RANK) ligand RANKL, tumour necrosis factor alpha (TNFα), interleukin 1 beta (IL1β) and Cluster of differentiation 40 ligand (CD40L) influence breast cancer - bone cell interactions[5-8]. Binding of these ligands to their respective receptors activates the canonical NFκB signalling pathway by initiating the recruitment of receptor-associated factors (TRAF) TRAF2 and TRAF6[6-8]. This in turn leads to the binding of IκB kinase (IKK) alpha (IKKα) and beta (IKKβ) to the regulatory subunit IKKγ[9, 10]. Once activated, the IKKαβγ complex phosphorylates and triggers the proteasomal degradation of IκB that results in NFκB nuclear translocation[6].

A number of studies have reported that mice deficient in NFκB1/2, TRAF2, TRAF6, IKKα or IKKβ exhibited high bone mass due to osteoclast inhibition[11-15]. Furthermore, pharmacological inhibition of NFκB activation reduced osteoclast number and protected against bone loss in models of inflammation and oestrogen deficiency[16-20]. NFκB activation is also involved in the regulation of osteoblast differentiation and bone formation. For example, TNFα and transforming growth factor beta (TGFβ) induces osteoblast apoptosis[1, 3, 21] and knockdown of IKK in osteoblasts and their precursors enhances bone nodule formation *in vitro* and stimulates bone formation in mice [22].

There is also evidence to suggest that NFκB regulates osteoclast and osteoblast activity through its crosstalk with the Wnt/β-catenin pathway[23]. In osteoblasts, activation of β-catenin stimulates

bone formation and enhances the expression of runt related transcription factor 2 (Runx2), a key osteogenic factor essential for osteoblast differentiation [24-27]. Activation of β-catenin inhibits osteoclast formation [28-30] and activation of NFκB by RANKL in osteoclasts leads to β-catenin inhibition [31, 32]. Altogether, these findings implicate the NFκB/β-catenin axis in the regulation of osteoclast and osteoblast activity and bone remodelling.

Over recent years, there has been increasing interest in the role of NFκB in the regulation of breast cancer bone metastasis [33, 34]. NFκB in breast cancer cells enhances osteoclast formation and promotes bone metastasis. Recent work carried out in our laboratories has shown that pharmacologic inhibitors of NFκB reduced osteolysis in a model of breast cancer osteolytic metastasis [33, 34]. However, the role of NFκB – and its interaction with β-catenin - in the regulation of osteoblast and osteoclast changes associated with breast cancer-induced osteolysis has not been investigated. Using a pharmacological approach that utilizes data from experiments using bone cells, organ cultures and immuno-competent mice, we showed that the sesquiterpene lactone Parthenolide (PTN), a verified inhibitor of NFκB[34-37], enhanced β-catenin expression and activity in osteoblasts and osteoclasts *in vitro*, and protected against breast cancer-induced osteolysis *ex vivo* and *in vivo*.

2. Materials and methods

2.1. Reagents and cells

The sesquiterpene lactone PTN was purchased from Tocris Biosciences (Bristol, UK). Parental and osteotropic clones of human MDA-MB-231 and mouse 4T1-BT1 (representative of triple-negative), human MCF7 (hormone sensitive breast cancer cell lines), and the osteoblast-like cells Saos-2 and MC3T3, and the macrophage-like cell (pre-osteoclasts) RAW 264.7 were purchased from ATCC (Manassas, VA). The osteotropic sub clones of the triple negative human MDA-231-BT1 and BT2 and mouse 4T1-BT1 and BT2 were generated by repeated passages *in vivo* and validated for their

ability to colonize bone and to cause osteolysis[38-40]. Tissue culture medium was obtained from Sigma-Aldrich (Dorset, UK). Primers for quantitative PCR were designed using the Roche website and obtained from Invitrogen (Paisley, UK) and probes were purchased from Roche Diagnostics Ltd. (East Sussex, UK). Antibodies were purchased from Cell Signalling Biotechnology (MA, USA) except rabbit anti-actin was obtained from Sigma-Aldrich (Dorset, UK). Mouse macrophage colony stimulating factor (M-CSF) was obtained from R&D Systems (Abingdon, UK) and RANK ligand (RANKL) was a gift from Patrick Mollat (Galapagos SASU, France)[16].

2.2. Animal experiments

All experimental protocols were approved by the Ethics Committee at the Universities of Edinburgh and Sheffield and were conducted in accordance with the UK Home Office regulations.

2.2.1. Intra-tibial injection in mice

Balb/c female mice (10-week-old) received intra-tibial injection of mouse 4T1-BT1 breast cancer cells (4×10^3 cells) in the left leg and a sham injection of PBS into their right leg. On day 2, animals were divided into two groups (7 mice per group) and received intraperitoneal injection of either vehicle (Dimethyl sulfoxide (DMSO)/water, 1:10) or PTN (10mg/kg/day) for 12 days. Treatment regime used was chosen based on previous *in vivo* studies, which demonstrated that this agent has anti-resorptive and anti-metastatic effects[34]. Animals were euthanized 14 days post injection of 4T1-BT1 cells and bone architecture was assessed by micro–computed tomography (microCT, Brucker 1172 scanner, Brucker, Belgium)[41]. Skeletal tumor growth was measured on 2D microCT images using Image J (1.34s; NIH, Bethesda, MD, USA) and results were expressed as a percentage of total metaphyseal area.

2.2.2. Supracalvarial injection in mice

C57BL/6 female mice (3-weeks-old) were divided into two groups (7 mice per group) and received intraperitoneal injection of either vehicle (DMSO/water, 1:10) or PTN (3mg/kg/day) for 6 days. On day 2, mice were injected subcutaneously over the calvarial bones (supra-calvarial) with 50μL of conditioned medium from human MDA-231-BT1, mouse 4T1-BT1 and human MCF7 breast cancer cells on 5 consecutive days[39]. Osteolytic bone loss in the calvarial bone was assessed using microCT at a resolution of 8μm[41]. All mice injected with conditioned medium from human MDA-231 or MCF7 or mouse 4T1 did not exhibit any obvious physical signs of illness or inflammatory response.

2.3. Micro-computed tomography

Trabecular bone parameters were measured at the left proximal tibia (200 slices distal of the growth plate) using microCT analysis (Skyscan 1172 instrument (Brucker, Belgium) set at 60kV and 150μA [41]. Images were reconstructed by the Skyscan NRecon program and analysed using Skyscan CTAn software (Brucker, Belgium) [41].

2.4. Bone histomorphometry

Bone histomorphometry was performed on the proximal tibial metaphysis from mice as previously described [34, 42]. Briefly bones were fixed, sectioned using a Leica microtome (Solms, Germany) and tissue sections were stained with von Kossa, Paragon, tartrate-resistant acid phosphatase (TRAcP) and aniline blue. Static and dynamic bone histomorphometry were performed on trabecular bone (0.1 and 1mm distal to the growth plate) and three sections per samples were analysed using computer software based on the Aphelion Image Analysis tool kit (Adcis, He0rouville- Saint-Clair, France).

2.5. Cancer cell – mouse calvaria organ co-culture system

The effects of pharmacological inhibition of NFκB on local osteolysis induced by human and mouse cancer cell derived factors was studied *ex vivo* using an adaptation of the mouse calvarial organ culture as described in[42]. Briefly, neonatal mouse calvarias were isolated from 7-day-old mice, divided into equal halves along the medium sagittal suture and each half was placed into culture on stainless steel rafts in 48-well plates containing standard or conditioned medium. Tissue culture medium containing test agents was changed every 48 hours and the cultures were terminated after 7 days. Bone volume was assessed by using microCT at a resolution of 5μm.

2.6. Osteoblast cultures

Primary osteoblasts were isolated from the calvarial bones of 2-day-old mice as previously described[43]. Primary calvarial osteoblasts or the osteoblast-like cells Saos-2 and MC3T3 were seeded into 12-well plates at 10 x 10^5 cells per well in standard alpha-MEM or DMEM respectively, supplemented with β-glycerol phosphate (10 μM) and L-ascorbic acid (50 μg/ml) for up to 21 days. Osteoblast cell number, differentiation and bone nodule formation were determined by AlamarBlue assay, alkaline phosphatase (Alk Phos) assay and alizarin red (ALZ) staining as previously described[43].

2.7. Osteoclast cultures

Bone marrow (BM) cells were flushed from the long bones of 3-5 month old mice and primary osteoblasts were isolated from the calvarial bones of 2-day-old mice as previously described[43]. Osteoblasts were plated in 96-well plates (8 x 10^3 cells/well) for 24 hours and BM cells were added (2x10^5 cells/well). M-CSF-dependent osteoclast precursor cells generated as previously described[42] and were plated into tissue culture plates (96 well plates, 15 x 10^3 cells/well; 12 well plates, 150 x 10^3 cells/well) in standard alpha-MEM supplemented with M-CSF (25 ng/ml) and RANKL (100 ng/ml). For studies involving breast cancer cells and their derived factors, M-CSF-dependent osteoclast precursors were plated into 96 well plates (15 x 10^3 cells / well) in alpha-

MEM supplemented with M-CSF (25 ng/ml) and RANKL (100 ng/ml) for 6 hours prior addition of MDA-231-BT1, 4T1-BT1 or MCF7 breast cancer cells (300 cells/well) or their conditioned medium (20% v/v) prepared as previously described [42]. Cultures were terminated by fixation in 4% paraformaldehyde, and stained for Tartrate-Resistant Acid Phosphatase (TRAcP). Resorption pits were visualised in osteoclast cultures plated on Corning® Osteo Assay Surface multiple well plates (Corning, USA) using an Olympus ScanR microscope and resorbed area was quantified by ImageJ.

2.8. Western Blotting

Western blot analysis was used to detect protein expression. Prior to stimulation with test agents or vehicle, cells were incubated in serum free medium for 60 minutes. Test agents or vehicle were added and cells were then gently scraped in standard lysis buffer (0.1% (w/v) SDS, 0.5% (w/v) sodium deoxycholate, 1% Triton X-100, 1μM EDTA, 2% (v/v) protease inhibitor cocktail, 10μM of sodium fluoride and 2% (v/v) phosphatase inhibitor cocktail) or cytoplasmic lysis buffer (10 mM Tris (pH 7.5), 100 mM NaCl, 0.05% NP-40, 3 mM MgCl2, 1 mM EGTA supplemented with 2% (v/v) protease and phosphatase inhibitor cocktail). Protein concentration was determined using BCA assay (Pierce, USA). Total protein (50 - 70μg) was resolved by SDS-PAGE (BioRAD, UK) and immunoblotted with antibodies according to manufacturer's instructions. Detection of native and phosphorylated proteins was performed using rabbit monoclonal antibodies (all at 1:1000 dilution, cell Signalling Technology, USA). Immuno-complexes were visualised by an enhanced chemiluminescence detection kit (Pierce, USA) using horseradish peroxidase-conjugated secondary antibody (Jackson labs, UK), and visualised using chemiluminescence (Amersham, UK) on a Syngene GeneGnome imaging system. The intensity of the bands was quantified using GeneSnap software (Syngene, UK) and level of actin (Sigma-Aldrich, UK) was used for normalization.

2.9. Quantitative PCR

Gene expression was detected using quantitative PCR (qPCR). Briefly, samples were lysed using TRIzol reagent and quantified using a nanodrop (Thermo Scientific) according to manufacturer's instructions. Complementary DNA (cDNA) was generated using Invitrogen SuperScript III Reverse Transcriptase kit according to manufacturer's instructions. Primers were designed using the Ensembl genome browser, and Roche website. For amplification of mouse OPG (forward primer: 5'- ATGAACAAGTGGCTGTGCTG-3', reverse primer 5'-CAGTTTCTGGGTCATAATGCAA-3'); mouse RANKL (forward primer: 5'-TGAAGACACACTACCTGACTCCTG-3', reverse primer 5'-CCACAATGTGTTGCAGTTCC -3'); mouse GAPDH (forward primer: 5'-CCTGAATTTTAAGCTACACACAGC -3', reverse primer 5'- CTGGCACTGCACAAGAAGAT -3'), mouse Runx2 (forward primer: 5'-CCACAAGGACAGAGTCAGATTACA-3', reverse primer 5'- TGGCTCAGATAGGAGGGGTA -3'); mouse alkaline phosphatase (ALP, AKP2 (ALPL)) (forward primer: 5'-AAGGCTTCTTCTTGCTGGTG-3', reverse primer 5'GCCTTACCCTCATGATGTCC -3') were used. Levels of gene expression were expressed as copy number per micro-gram of total RNA and GAPDH was used for cDNA normalization.

2.10. Transcription factors assays

Nuclear extracts from cultures of mouse M-CSF dependent osteoclast precursors and osteoblasts were prepared using a nuclear extract kit (Active Motif, Rixensart, Belgium) and DNA binding was measured using TRANSAM ELISA kit for p65 NFκB and c-Fos (Active Motif, Rixensart, Belgium), according to the manufacturer's instructions.

2.11. Immunostaining for NFκB

Mature osteoclasts were generated in M-CSF and RANKL-stimulated mouse bone marrow cultures as described above. Cultures were permeabilised in Triton X100 (0.1% v/v), stained with rabbit anti-p65 NFκB (1:200, Santa Cruz Biotechnology, Dallas, USA) and Alexafluor488-conjugated goat–anti-Rabbit antibody (1:200, Fisher Scientific UK, Loughborough, UK) and counterstained

with DAPI (4',6-Diamidino-2-Phenylindole, Dihydrochloride). Cytoplamic and nuclear staining of p65NFκB was visualised using a fluorescence microscope (Zeiss, Cambridge, UK).

2.12. Statistical analysis

Comparison between groups was assessed by analysis of variance (ANOVA) followed by Dunnet's post hoc test (SPSS for Windows, version 11). A p-value value of 0.05 or below was considered statistically significant. The half maximal inhibitory concentration (IC50) values were calculated using GraphPad Prism 4 for windows (V10, Microsoft, USA).

3. Results

3.1. Effects of NFκB inhibition on the growth osteotropic breast cancer cells *in vitro*

Previous studies have shown that NFκB inhibition reduced the growth of parental breast cancer cell lines [5, 44]. In view of the fact that breast cancer cells in the skeleton (osteotropic) exhibit an altered phenotype compared to their parental counterpart, we assessed the cytotoxic effect of the NFκB inhibitor PTN against a panel of osteotropic, triple-negative (human MDA-231-BT1/2 and mouse 4T1-BT1/2) and estrogen receptor positive (human MCF7) breast cancer cell lines[38-40]. PTN reduced the growth of all cell lines tested in a concentration-dependent manner (Fig. S1). The concentration of PTN that half maximally inhibited cell viability (IC50) was significantly lower in osteotropic cells when compared to their parental control (Table 1). In contrast, PTN had no significant effects on the growth of osteoblasts or bone marrow derived osteoclast precursors at concentrations up to 10μM (Table 1).

3.2. PTN reduces osteoblast support for osteoclastogenesis

Cells of the osteoblast lineage contribute to breast cancer-induced osteolysis through secretion of various osteoclastic factors including RANKL[3, 4, 45]. In this study, we utilized *ex vivo* organ and *in vitro* osteoblast culture systems to test the effects of NFκB inhibition on osteoblast support for osteoclastogenesis in the presence of breast cancer cells or their derived factors. In cancer cell -

calvarial organ co-culture, PTN (1μM) inhibited osteoclast formation (Fig. 1A, left panel and Fig. S2A) and osteolysis (Fig. 1A, right panel and Fig. 1B) induced by MDA-231-BT1, 4T1-BT1 and MCF7 breast cancer cells. Addition of conditioned medium from these cells to calvarial osteoblast – bone marrow co-cultures enhanced osteoclast formation and these effects were significantly inhibited in the presence of PTN (1μM) (Fig. 1C). Representative photomicrographs of osteoclasts from the experiment described are shown in Fig. S2B. Pretreatment of calvarial osteoblasts with PTN (5μM) prior to the addition of condition medium from the osteotropic MDA-231-BT1 cells significantly inhibited RANKL/OPG ratio after 24 hours (Fig. 1D). Collectively, these results demonstrate that PTN inhibits osteolysis by disrupting breast cancer – osteoblast – osteoclast crosstalk in the models described.

3.3. PTN enhances osteoblast proliferation, differentiation and bone nodule formation

In view of previous findings that showed that NFκB inhibition in osteoblasts enhances bone formation[24], we examined the effects of PTN on osteoblast proliferation, differentiation and bone nodule formation in the presence and absence of breast cancer derived factors. Treatment of mouse calvarial osteoblasts with PTN (0.01μM) increased alkaline phosphatase activity within 24 hours (Fig. 2A, left panel) and enhanced bone nodule bone formation after 21 days (Fig. 2B, left panel) ($p<0.01$). Representative photomicrographs of bone nodule formation from the experiment described are shown in Fig. 2C. Exposure of mouse calvarial osteoblasts to conditioned medium from human MDA-231-BT1 breast cancer cells inhibited alkaline phosphatase activity after 24 (Fig. 2A, middle panel) and reduced bone nodule bone formation after 14 days (Fig. 2B, middle panel). These effects were completely inhibited by PTN (0.01 – 0.1μM) ($p < 0.01$). Interestingly, conditioned medium from osteotropic 4T1 enhanced alkaline phosphatase activity (Fig. 2A, right panel) in osteoblast cultures. Treatment with PTN (0.01 – 0.1μM) had no effects on alkaline

phosphatase activity (Fig. 2A, right panel) in these cultures, but PTN further enhanced the increase in bone nodule formation caused by exposure to conditioned medium from 4T1-BT1 (Fig. 2B, right panel). A similar increase in alkaline phosphatase activity (Fig. S3A) and bone nodule formation (Fig. S3B) was observed in cultures of the osteoblast-like cells MC3T3 treated with PTN for 7 days. In addition, exposure of osteoblasts to PTN (0.1μM) increased the mRNA expression of alkaline phosphatase and Runx2 after 24 and 72 hours (Fig. 2D), consistent with enhanced alkaline phosphatase activity and osteoblast differentiation.

3.4. NFκB inhibition by PTN enhances β-catenin activation and expression in osteoblasts

Mechanistic studies in calvarial osteoblasts showed that pretreatment with PTN (5μM) for 1 hour prior to addition of conditioned medium from human MDA-231-BT1 or mouse 4T1-BT1 prevented IκB phosphorylation after 15 minutes (Fig. 3A-B), inhibited NFκB DNA binding after 45 minutes (Fig. 3C) and reduced β-catenin cytoplasmic sequestration and increased its nuclear translocation (Fig. 3D-E) after 3 hours. Exposure of osteoblasts to PTN (1μM) for 24 hours enhanced β-catenin protein level and reduced the expression of IκB (Fig. 3F). These results suggest that the NFκB inhibitor PTN enhances β-catenin activation in osteoblast in the presence of breast cancer derived factors.

3.5. Disruption of the NFκB/β-catenin pathway by PTN in osteoclasts reduces breast cancer-induced osteoclastogenesis

Next, we tested the effects of PTN on breast cancer-induced osteoclastogenesis in the absence of osteoblasts. As shown in Fig. 4 (panels A and B), exposure of mouse M-CSF generated osteoclast precursors to the breast cancer cells MDA-231-BT1, MCF7 and 4T1-BT1 or their derived factors enhanced RANKL-induced osteoclast formation ($p < 0.001$), and these effects were inhibited by PTN in a concentration dependent manner (IC50; 0.13 ± 0.1 for MDA-231-BT1, 0.53 ± 0.2 for 4T1-BT1 and 4.17 ± 1.2 for MCF7 cells). Representative photomicrographs of osteoclasts from the

experiment described are shown in Fig. S2C. Of note, PTN had no effects on the proliferation of M-CSF generated osteoclast precursors (Fig. S2D-E). This excludes the possibility that the inhibitory effect on osteoclast formation was mediated by a reduction in pre-osteoclast cell number. Mechanistic studies in osteoclast precursors showed that exposure to PTN (5μM) for 1 hour inhibited IκB phosphorylation (Fig. 4C) and p65NFκB DNA binding (Fig. 4D) induced by RANKL (100ng/ml) or conditioned medium. Representative microphotographs of p65NFκB nuclear translocation in osteoclasts in the presence and absence of PTN (10μM) are shown in Fig. S4. Additionally, exposure to RANKL (100ng/ml) reduced β-catenin and IκB expression in osteoclast precursor-like cells RAW 264.7 after 48 hours (Fig. 4F), and these effects were reversed by pretreatment with PTN (1μM) (Fig. 4E-F). Collectively, these results demonstrate that pharmacological disruption of NFκB - and its interaction with β-catenin - in osteoclasts by PTN inhibits RANKL and breast cancer cell support for osteoclastogenesis.

3.6. PTN induces osteoclast apoptosis

Mature osteoclast survival is a major determinant of osteolytic bone loss [46]. With this in mind, we examined the effects of PTN on osteoclast survival and apoptosis. We generated mature osteoclasts and then exposed these cells to PTN in the presence and absence of M-CSF, RANKL or conditioned medium from human MDA-231-BT1 cells. As shown in Fig. 5 (panel A), exposure of osteoclasts to conditioned medium from MDA-231-BT1 cells (20% v/v) reduced osteoclast death due to withdrawal of M-CSF (25ng/ml) or RANKL (100ng/ml). Treatment with PTN (0.1 - 1μM) exacerbated osteoclast inhibition in these cultures after 24 hours of continuous treatment (Fig. 5A). PTN also induced caspase-3/7 activation in mature osteoclasts after 6 hours (Fig. 5B) and caused osteoclast apoptosis after 24 hours (Fig. 5C), as evident by nuclear condensation and DNA fragmentation as assessed by DAPI and TUNEL assays, respectively. Osteoclast apoptosis in these

cultures was significantly inhibited in the presence of the Caspase inhibitor zVAD-fmk (Fig. 5D), indicative of caspase involvement. We also investigate the effects of PTN on osteoclast activity in the presence and absence of conditioned medium (10% v/v) from MDA-231-BT1. The results of this experiment showed that exposure of mature osteoclasts to MDA-231-BT1 cells significantly increased bone resorption, and this was not affected by PTN treatment (1μM) (Fig. S5).

3.7. PTN reduces breast cancer related osteolysis

We tested the effects of PTN on osteolytic bone damage caused by breast cancer cells or their derived factors in immuno-competent mice (Fig. 6A). Administration of PTN (3mg/kg/3-weekly) in immuno-competent mice 24 hours prior to supra-calvarial injection of conditioned medium from human MDA-231-BT1, MCF7 and mouse 4T1-BT1 breast cancer cells increased bone volume (Fig. 6B). Next, we examined the effects of PTN on skeletal tumour growth and bone loss in the syngeneic 4T1 model of osteolysis. PTN (10mg/kg/3-weekly) was administered in mice 1 day prior to intra-tibial injection of the osteotropic 4T1-BT1 (4×10^3) and continued to day 12 (Fig. 6C). All mice that were treated with vehicle (0.01% DMSO) developed local osteolysis, characterised by a significant loss in trabecular bone volume (% BV/TV), thickness (% Tb.Th) and connectivity (% Conn.D) (Fig. 6D). These changes were significantly inhibited by treatment with PTN (10mg/kg/3-weekly). Detailed microCT analysis of tumor growth in the metaphysis of the proximal tibia showed that PTN reduced the size of lytic lesions (Fig. 6E), indicative of reduced tumour area. Further histomorphometric analysis of bone revealed that PTN reduced osteoclast number (Oc.N/BS, Fig. 6F, left panel), suppressed osteoclast activity (Oc.S/BS, Fig. 6F, right panel) and enhanced osteoblast number (Ob.N/BS, Fig. G, left panel), without affecting active osteoblast surface (Ob.S/BS, Fig. 6G, middle panel) and width (Ob.W, Fig. 6G, right panel).

4. Discussion

Breast cancer cells frequently metastasize to the skeleton in patients with secondary breast cancer [1-3]. Osteoclast and osteoblast activity in the tumour microenvironment plays an essential role in the regulation of breast cancer cell behaviour in the skeleton[1-4]. The NFκB signalling pathway regulates osteoclast and osteoblast differentiation in health and disease[16, 34, 47]. Previous studies have also implicated NFκB in the initiation and progression of bone metastasis [33, 34], and pharmacological inhibitors of NFκB reduced breast cancer-induced osteolysis [33, 34]. However, the bone-autonomous contribution of NFκB to breast cancer-induced osteolysis is poorly understood. This and the fact that most previous studies that have implicated NFκB in bone metastasis were performed in immuno-deficient mice have led us to study the bone cell-autonomous contribution of NFκB to breast cancer related bone cell activity and osteolysis *in vitro*, *ex vivo* and in immuno-competent mice.

Previous studies showed that NFκB inhibition reduced osteolysis and this effect was attributed – at least in part - to the reduction in number of breast cancer cells metastasizing to bone [33, 34]. Here, we provide pharmacological evidence to show that bone cell-specific inhibition of NFκB by PTN reduced osteolysis induced by conditioned medium from human and mouse breast cancer cells. Data from *in vitro* bone cell and organ cultures and histomorphometric analysis of bone confirmed that this agent inhibited breast cancer- and RANKL-induced osteoclast formation and reduced the ability of breast cancer cells to prolong osteoclast survival and to inhibit osteoclast apoptosis. It is important to note however that this agent had no direct effect on bone resorption by mature osteoclasts at concentrations that do not affect osteoclast survival (Fig. S5A-C). Breast cancer- and bone-derived mediators other than RANKL are implicated in the regulation of breast cancer – bone cell interactions [3, 4]. In this study, we show that PTN also inhibited NFκB activation by TNFα and TGFβ in cultures of osteoclasts and their precursors that have been primed with MDA-

231-BT1 conditioned medium (Fig. S6). These findings are entirely consistent with the pro-apoptotic and anti-resorptive effects of this agent, and of great interest in demonstrating that NFκB inhibition suppresses excessive osteoclast formation caused by RANKL, breast cancer cells and other osteolytic mediators such as TNFα and TGFβ that are often present in the bone tumour microenvironment.

Osteolysis supports the growth of metastatic breast cancer cells in the skeleton [1-3]. Previous studies have shown that breast cancer cells in the skeleton exhibit an altered phenotype compared to their parental counterpart [1-4]. Here, we show that osteotropic sub-clones of the human MDA-231 and mouse 4T1 breast cancer cells were sensitive to treatment with PTN when compared to parental cells. Furthermore, PTN inhibited tumour area in mice injected with the osteotropic 4T1-BT cells, suggesting an anti-tumour effect. Whilst we cannot exclude the possibility that PTN exerts a direct inhibitory effect on tumor growth *in vivo*, it is likely that the anti-tumour effect observed in our *in vivo* model was mainly due to osteoclast inhibition. Evidence to support this hypothesis comes from the anti-osteoclast effects observed *in vitro, ex vivo* and *in vivo*, and from *in vitro* studies that showed that the concentrations of PTN that needed to inhibit growth of breast cancer cells were at least 10 times higher than those that inhibited osteoclast formation.

NFκB inhibition is associated with increased osteoblast differentiation and maturation[22]. With this in mind, we examined the effects of PTN on osteoblast differentiation and activity in the presence and absence of conditioned medium from human and mouse breast cancer cells [21, 22, 27]. PTN reduced osteoblast inhibition by breast cancer cells, as evidenced by marked increase in osteoblast differentiation and bone nodule formation, and also by the fact that PTN enhanced ALP expression and activity, increased Runx-2 expression and stimulated β-catenin activation in osteoblasts. Moreover, PTN had no effects on osteoblast apoptosis in the presence or absence of

conditioned medium from breast cancer cells (data not shown). It is important to note however that administration of PTN in mice stimulated osteoblast number but had no significant effects on bone formation rate in the 4T1 model described. Future *in vivo* studies in models of osteolysis are needed to evaluate the consequences and implications of osteoblast stimulation by PTN in the treatment of breast cancer bone metastasis.

NFκB cooperates with multiple signaling pathways in bone and breast cancer cells [32]. One of the transcription factors that is essential for osteoclast formation is c-Fos [48]. In this study, we showed that exposure of osteoclasts and their precursors to PTN reduced the phosphorylation and DNA binding of c-Fos by TNFα-, RANKL- or MDA-231-BT1 conditioned medium (Fig. S7). Previous studies have implicated β-catenin in the stabilization and cytoplasmic sequestration of p65NFκB[32]. Wnt/β-catenin signalling plays a role in the regulation of osteoclast and osteoblast differentiation, and Sclerostin, a secreted inhibitor of Wnt/β-catenin signalling reduces bone formation[25-27, 32]. In broad agreement with these findings, we showed that NFκB inhibition by PTN in osteoblasts and osteoclasts was accompanied by a significant increase in β-catenin activation and expression. Notwithstanding this, we cannot exclude the involvement of other mechanisms since PTN has been reported to affect a wide array of cellular processes including DNA methylation and generation of reactive oxygen species[37].

In conclusion, our present data together with previous results obtained from immuno-deficient mice [33, 34] suggest that NFκB plays a key role in the regulation of breast cancer-induced bone cell activity and osteolysis. We also presented pharmacological evidence to suggest that bone-specific inhibition of NFκB suppresses osteoclast formation and reduces osteoblast inhibition related to breast cancer by engaging β-catenin signalling. When combined with previous studies[32], our

present results raise the possibility that combined targeting of NFκB and β-catenin signalling may be of value in the treatment of breast cancer associated bone disease.

5. Acknowledgements

This work was supported in part by a pump-prime grant from Cancer Research UK (University of Edinburgh) and Breast Cancer Now (University of Sheffield) grants to Aymen I. Idris.

6. Conflict of Interest

Patrick Mollat is an employee of Galapagos SASU (102 Avenue Gaston Roussel, 93230 Romainville, France).

7. References:

[1] G.R. Mundy, Metastasis to bone: causes, consequences and therapeutic opportunities, Nat.Rev.Cancer, 2 (2002) 584-593.

[2] R.E. Coleman, Metastatic bone disease: clinical features, pathophysiology and treatment strategies, Cancer Treat.Rev., 27 (2001) 165-176.

[3] G.D. Roodman, Mechanisms of bone metastasis, N.Engl.J.Med., 350 (2004) 1655-1664.

[4] V.A. Siclari, T.A. Guise, J.M. Chirgwin, Molecular interactions between breast cancer cells and the bone microenvironment drive skeletal metastases, Cancer Metastasis Rev., 25 (2006) 621-633.

[5] M. Karin, Y. Cao, F.R. Greten, Z.W. Li, NF-kappaB in cancer: from innocent bystander to major culprit, Nature reviews. Cancer, 2 (2002) 301-310.

[6] X. Feng, RANKing intracellular signaling in osteoclasts, IUBMB.Life, 57 (2005) 389-395.

[7] J. Gohda, T. Akiyama, T. Koga, H. Takayanagi, S. Tanaka, J. Inoue, RANK-mediated amplification of TRAF6 signaling leads to NFATc1 induction during osteoclastogenesis, EMBO J., 24 (2005) 790-799.

[8] J. Mizukami, G. Takaesu, H. Akatsuka, H. Sakurai, J. Ninomiya-Tsuji, K. Matsumoto, N. Sakurai, Receptor activator of NF-kappaB ligand (RANKL) activates TAK1 mitogen-activated protein kinase kinase kinase through a signaling complex containing RANK, TAB2, and TRAF6, Mol.Cell Biol., 22 (2002) 992-1000.

[9] J.Y. Chung, Y.C. Park, H. Ye, H. Wu, All TRAFs are not created equal: common and distinct molecular mechanisms of TRAF-mediated signal transduction, J.Cell Sci., 115 (2002) 679-688.

[10] S. Kishida, H. Sanjo, S. Akira, K. Matsumoto, J. Ninomiya-Tsuji, TAK1-binding protein 2 facilitates ubiquitination of TRAF6 and assembly of TRAF6 with IKK in the IL-1 signaling pathway, Genes Cells, 10 (2005) 447-454.

[11] M.A. Lomaga, W.C. Yeh, I. Sarosi, G.S. Duncan, C. Furlonger, A. Ho, S. Morony, C. Capparelli, G. Van, S. Kaufman, H.A. van der, A. Itie, A. Wakeham, W. Khoo, T. Sasaki, Z. Cao, J.M. Penninger, C.J. Paige, D.L. Lacey, C.R. Dunstan, W.J. Boyle, D.V.

Goeddel, T.W. Mak, TRAF6 deficiency results in osteopetrosis and defective interleukin-1, CD40, and LPS signaling, Genes Dev., 13 (1999) 1015-1024.
[12] B. Lamothe, W.K. Webster, A. Gopinathan, A. Besse, A.D. Campos, B.G. Darnay, TRAF6 ubiquitin ligase is essential for RANKL signaling and osteoclast differentiation, Biochem.Biophys.Res.Commun., 359 (2007) 1044-1049.
[13] J.E. Otero, S. Dai, M.A. Alhawagri, I. Darwech, Y. Abu-Amer, IKKbeta activation is sufficient for RANK-independent osteoclast differentiation and osteolysis, J.Bone Miner.Res., 25 (2010) 1282-1294.
[14] M.G. Ruocco, S. Maeda, J.M. Park, T. Lawrence, L.C. Hsu, Y. Cao, G. Schett, E.F. Wagner, M. Karin, I{kappa}B kinase (IKK){beta}, but not IKK{alpha}, is a critical mediator of osteoclast survival and is required for inflammation-induced bone loss, J Exp.Med., 201 (2005) 1677-1687.
[15] M.L. Chaisson, D.G. Branstetter, J.M. Derry, A.P. Armstrong, M.E. Tometsko, K. Takeda, S. Akira, W.C. Dougall, Osteoclast differentiation is impaired in the absence of inhibitor of kappa B kinase alpha, J.Biol.Chem., 279 (2004) 54841-54848.
[16] A.I. Idris, M. Krishnan, P. Simic, E. Landao-Bassonga, P. Mollat, S. Vukicevic, S.H. Ralston, Small molecule inhibitors of I{kappa}B kinase signaling inhibit osteoclast formation in vitro and prevent ovariectomy-induced bone loss in vivo, FASEB J., 24 (2010) 4545-4555.
[17] K.W. McIntyre, D.J. Shuster, K.M. Gillooly, D.M. Dambach, M.A. Pattoli, P. Lu, X.D. Zhou, Y. Qiu, F.C. Zusi, J.R. Burke, A highly selective inhibitor of I kappa B kinase, BMS-345541, blocks both joint inflammation and destruction in collagen-induced arthritis in mice, Arthritis Rheum., 48 (2003) 2652-2659.
[18] S. Dai, T. Hirayama, S. Abbas, Y. Abu-Amer, The IkappaB kinase (IKK) inhibitor, NEMO-binding domain peptide, blocks osteoclastogenesis and bone erosion in inflammatory arthritis, The Journal of biological chemistry, 279 (2004) 37219-37222.
[19] E. Jimi, K. Aoki, H. Saito, F. D'Acquisto, M.J. May, I. Nakamura, T. Sudo, T. Kojima, F. Okamoto, H. Fukushima, K. Okabe, K. Ohya, S. Ghosh, Selective inhibition of NF-kappa B blocks osteoclastogenesis and prevents inflammatory bone destruction in vivo, Nat Med, 10 (2004) 617-624.

[20] Y. Zhang, H. Guan, J. Li, Z. Fang, W. Chen, F. Li, Amlexanox Suppresses Osteoclastogenesis and Prevents Ovariectomy-Induced Bone Loss, Scientific reports, 5 (2015) 13575.

[21] R.R. Mercer, C. Miyasaka, A.M. Mastro, Metastatic breast cancer cells suppress osteoblast adhesion and differentiation, Clinical & experimental metastasis, 21 (2004) 427-435.

[22] B.F. Boyce, Z. Yao, L. Xing, Functions of nuclear factor kappaB in bone, Ann N Y Acad Sci, 1192 (2010) 367-375.

[23] V. Krishnan, H.U. Bryant, O.A. MacDougald, Regulation of bone mass by Wnt signaling, J Clin.Invest, 116 (2006) 1202-1209.

[24] J. Chang, Z. Wang, E. Tang, Z. Fan, L. McCauley, R. Franceschi, K. Guan, P.H. Krebsbach, C.Y. Wang, Inhibition of osteoblastic bone formation by nuclear factor-kappaB, Nat.Med., 15 (2009) 682-689.

[25] J. Chang, F. Liu, M. Lee, B. Wu, K. Ting, J.N. Zara, C. Soo, K. Al Hezaimi, W. Zou, X. Chen, D.J. Mooney, C.Y. Wang, NF-kappaB inhibits osteogenic differentiation of mesenchymal stem cells by promoting beta-catenin degradation, Proc Natl Acad Sci U S A, 110 (2013) 9469-9474.

[26] C. Le Henaff, R. Mansouri, D. Modrowski, M. Zarka, V. Geoffroy, C. Marty, N. Tarantino, E. Laplantine, P.J. Marie, Increased NF-kappaB Activity and Decreased Wnt/beta-Catenin Signaling Mediate Reduced Osteoblast Differentiation and Function in DeltaF508 Cystic Fibrosis Transmembrane Conductance Regulator (CFTR) Mice, The Journal of biological chemistry, 290 (2015) 18009-18017.

[27] D. Mendoza-Villanueva, L. Zeef, P. Shore, Metastatic breast cancer cells inhibit osteoblast differentiation through the Runx2/CBFbeta-dependent expression of the Wnt antagonist, sclerostin, Breast cancer research : BCR, 13 (2011) R106.

[28] W. Wei, D. Zeve, J.M. Suh, X. Wang, Y. Du, J.E. Zerwekh, P.C. Dechow, J.M. Graff, Y. Wan, Biphasic and dosage-dependent regulation of osteoclastogenesis by beta-catenin, Mol Cell Biol, 31 (2011) 4706-4719.

[29] K. Otero, M. Shinohara, H. Zhao, M. Cella, S. Gilfillan, A. Colucci, R. Faccio, F.P. Ross, S.L. Teitelbaum, H. Takayanagi, M. Colonna, TREM2 and beta-catenin regulate

bone homeostasis by controlling the rate of osteoclastogenesis, J Immunol, 188 (2012) 2612-2621.

[30] J. Albers, J. Keller, A. Baranowsky, F.T. Beil, P. Catala-Lehnen, J. Schulze, M. Amling, T. Schinke, Canonical Wnt signaling inhibits osteoclastogenesis independent of osteoprotegerin, The Journal of cell biology, 200 (2013) 537-549.

[31] Y. Matsumoto, J. Larose, O.A. Kent, M. Lim, A. Changoor, L. Zhang, Y. Storozhuk, X. Mao, M.D. Grynpas, F. Cong, R. Rottapel, RANKL coordinates multiple osteoclastogenic pathways by regulating expression of ubiquitin ligase RNF146, The Journal of clinical investigation, 127 (2017) 1303-1315.

[32] Q. Du, D.A. Geller, Cross-Regulation Between Wnt and NF-kappaB Signaling Pathways, For Immunopathol Dis Therap, 1 (2010) 155-181.

[33] B.K. Park, H. Zhang, Q. Zeng, J. Dai, E.T. Keller, T. Giordano, K. Gu, V. Shah, L. Pei, R.J. Zarbo, L. McCauley, S. Shi, S. Chen, C.Y. Wang, NF-kappaB in breast cancer cells promotes osteolytic bone metastasis by inducing osteoclastogenesis via GM-CSF, Nat.Med., 13 (2007) 62-69.

[34] A.I. Idris, H. Libouban, H. Nyangoga, E. Landao-Bassonga, D. Chappard, S.H. Ralston, Pharmacologic inhibitors of IkappaB kinase suppress growth and migration of mammary carcinosarcoma cells in vitro and prevent osteolytic bone metastasis in vivo, Molecular cancer therapeutics, 8 (2009) 2339-2347.

[35] B.H. Kwok, B. Koh, M.I. Ndubuisi, M. Elofsson, C.M. Crews, The anti-inflammatory natural product parthenolide from the medicinal herb Feverfew directly binds to and inhibits IkappaB kinase, Chem.Biol., 8 (2001) 759-766.

[36] S.P. Hehner, T.G. Hofmann, W. Droge, M.L. Schmitz, The antiinflammatory sesquiterpene lactone parthenolide inhibits NF-kappa B by targeting the I kappa B kinase complex, J.Immunol., 163 (1999) 5617-5623.

[37] A. Ghantous, H. Gali-Muhtasib, H. Vuorela, N.A. Saliba, N. Darwiche, What made sesquiterpene lactones reach cancer clinical trials?, Drug discovery today, 15 (2010) 668-678.

[38] N. Rucci, E. Ricevuto, C. Ficorella, M. Longo, M. Perez, G.C. Di, A. Funari, A. Teti, S. Migliaccio, In vivo bone metastases, osteoclastogenic ability, and phenotypic characterization of human breast cancer cells, Bone, 34 (2004) 697-709.

[39] J.G. Logan, A. Sophocleous, S. Marino, M. Muir, V.G. Brunton, A.I. Idris, Selective tyrosine kinase inhibition of insulin-like growth factor-1 receptor inhibits human and mouse breast cancer-induced bone cell activity, bone remodeling, and osteolysis, Journal of bone and mineral research : the official journal of the American Society for Bone and Mineral Research, 28 (2013) 1229-1242.

[40] A.A. Rose, F. Pepin, C. Russo, J.E. Abou Khalil, M. Hallett, P.M. Siegel, Osteoactivin promotes breast cancer metastasis to bone, Mol.Cancer Res., 5 (2007) 1001-1014.

[41] G.M. Campbell, A. Sophocleous, Quantitative analysis of bone and soft tissue by micro-computed tomography: applications to ex vivo and in vivo studies, BoneKEy reports, 3 (2014) 564.

[42] A. Sophocleous, S. Marino, J.G. Logan, P. Mollat, S.H. Ralston, A.I. Idris, Bone cell-autonomous contribution of type 2 cannabinoid receptor to breast cancer induced osteolysis, The Journal of biological chemistry, (2015).

[43] S.E. Taylor, M. Shah, I.R. Orriss, Generation of rodent and human osteoblasts, BoneKEy reports, 3 (2014) 585.

[44] G. Sethi, K.S. Ahn, M.K. Pandey, B.B. Aggarwal, Celastrol, a novel triterpene, potentiates TNF-induced apoptosis and suppresses invasion of tumor cells by inhibiting NF-kappaB-regulated gene products and TAK1-mediated NF-kappaB activation, Blood, 109 (2007) 2727-2735.

[45] T. Suda, N. Takahashi, N. Udagawa, E. Jimi, M.T. Gillespie, T.J. Martin, Modulation of osteoclast differentiation and function by the new members of the tumor necrosis factor receptor and ligand families, Endocr.Rev., 20 (1999) 345-357.

[46] S.L. Teitelbaum, M.M. Tondravi, F.P. Ross, Osteoclasts, macrophages, and the molecular mechanisms of bone resorption, J Leukoc.Biol., 61 (1997) 381-388.

[47] J.Y. Kim, Y.H. Cheon, K.H. Yoon, M.S. Lee, J. Oh, Parthenolide inhibits osteoclast differentiation and bone resorbing activity by down-regulation of NFATc1 induction and c-Fos stability, during RANKL-mediated osteoclastogenesis, BMB reports, 47 (2014) 451-456.

[48] Z.Q. Wang, C. Ovitt, A.E. Grigoriadis, U. Mohle-Steinlein, U. Ruther, Wagner, Ef, Bone and haematopoietic defects in mice lacking c-fos, Nature, 360 (1992) 741-745.

Table I

Effects of Parthenolide on the growth of osteotropic breast cancer cells *in vitro*.

	Cell viability (IC_{50}, μM)
MDA-231	10.57 ± 0.15
MDA-231-BT1	8.17 ± 0.62
MDA-231-BT2	7.82 ± 0.69
MCF7	12.7 ± 1.10
4T1	6.79 ± 0.18
4T1-BT1	5.72 ± 0.61
4T1-BT2	1.90 ± 0.56
Pre-Osteoclasts	> 10
Osteoblasts	> 10

Cell viability was measured after 48 hours of continuous exposure to PTN by AlamarBlue assay. Calculation of half maximal inhibitory concentrations (IC50) has been performed as described under "Materials and Methods". Values are mean ± SD and are obtained from 5 independent experiments. BT denotes osteotropic tropic cells, and pre-osteoclasts refers to M-CSF generated osteoclast precursor cells.

Figure legends:

Fig. 1. PTN reduces osteoblast support for osteoclastogenesis. (A) *Ex vivo* osteoclast number and bone resorption in mouse calvarial organ culture exposed to conditioned medium (20% v/v) from human MDA-231-BT1 and MCF7 or mouse 4T1-BT1 cancer cells in the presence and absence of PTN (1μM). (B) Representative photomicrographs of osteolytic bone damage from the experiment described in panel A. (C) *In vitro* osteoclast formation in mouse calvarial osteoblast - bone marrow cell co-cultures after exposure to conditioned medium (CM, 20% v/v) from human MDA-231-BT1 and MCF7 or mouse 4T1-BT1 cancer cells in the presence and absence of PTN (1μM). (D) mRNA expression of RANKL and OPG in mouse calvarial osteoblasts exposed to conditioned medium (20% v/v) from human MDA-231-BT1 breast cancer cells in the presence and absence of PTN (5μM). Values are mean ± SD; * $p<0.05$ and ** $p<0.01$ from vehicle; + $p<0.05$ from vehicle plus breast cancer cells or conditioned medium.

Fig. 2. PTN enhances osteoblast differentiation and protects against osteoblast inhibition by breast cancer cells. (A-B) *In vitro* osteoblast differentiation (A) and bone nodule formation (B) in mouse calvarial osteoblast cultures exposed to standard or conditioned medium (20%v/v) from human MDA-231-BT1 or mouse 4T1-BT1 cancer cells in the presence or absence of PTN for 24 hours. (C) *In vitro* bone nodule formation in mouse calvarial osteoblasts (21 days) and Saos2 (10 days) treated with PTN at the indicated concentration in the presence and absence of conditioned medium from MDA-231-BT1 and 4T1-BT1. Osteoblast differentiation and bone nodule formation were assessed by Alkaline phosphatase (ALP) and Alazarin Red assays. (C) Representative photomicrographs of osteoblasts and bone nodule formation from the experiment described in panel B. (D) mRNA expression of ALP and Runx2 in mouse calvarial osteoblasts after 24 and 72 hours in

the presence or absence of PTN (0.1μM). Values are mean ± SD; * $p<0.05$ and + $p<0.05$ from vehicle plus breast cancer cell conditioned medium.

Fig. 3. PTN activates β-catenin signalling in osteoblasts. (A-B) Western blot analysis (A) and quantification (B) of total and phosphorylated IκB in mouse calvarial osteoblast cultures pretreated with vehicle or PTN (5μM) for 1 hour and exposed to conditioned medium 20%v/v) from human MDA-231-BT1 or mouse 4T1-BT1 cancer cells for 15 minutes. (C) NFκB DNA binding in mouse calvarial osteoblasts cultures pretreated with vehicle or PTN (5μM) for 1 hour and exposed to conditioned medium (20% v/v) from human MDA-231-BT1 (left) or mouse 4T1-BT1 (right) cancer cells for 45 minutes. (D-E) Western blot analysis (D) and quantification (E) of β-catenin expression in cytoplasm (Cyt) and nuclear (Nuc) fractions obtained from mouse calvarial osteoblasts cultures pretreated with vehicle or PTN (5μM) for 1 hour and exposed to standard medium or conditioned medium (20%v/v) from human MDA-231-BT1 breast cancer cells for 3 hours. (F) Differential expression of β-Catenin and IκB obtained from mouse calvarial osteoblast cultured in the presence or absence of PTN at the indicated concentration for 24 hours. Values are mean ± SD; * $p<0.05$ and ** $p<0.01$ from vehicle; + $p<0.05$ from vehicle plus breast cancer cell conditioned medium.

Fig. 4. PTN inhibits breast cancer cell- and RANKL-induced osteoclast formation. (A-B) *In vitro* osteoclastogenesis of murine M-CSF (25ng/ml) and RANKL (100ng/ml) stimulated bone marrow treated with vehicle or PTN (5μM) in the presence and absence of breast cancer cells (A) or their conditioned medium (20%v/v) (B) for 48 hours. (C) Western blot analysis of total and phosphorylated IκB in cultures of M-CSF (25ng/ml) dependent pre-osteoclasts after exposure to human RANKL (100ng/ml), human M-CSF (25ng/ml) or conditioned medium (20% v/v) from human MDA-231-BT1, 4T1-BT1 and MCF7 cancer cells in the presence and absence of PTN (5μM). (D) NFκB DNA binding in cultures of M-CSF (25ng/ml) dependent pre-osteoclasts

described in panel C. (E-F) Differential expression of β-Catenin and IκB in mouse RAW 264.7 macrophage (pre-osteoclasts) pretreated with vehicle or PTN (1μM) for 1 hour and cultured in the presence or absence of RANKL (100ng/ml) for 48 hours. Values are mean ± SD; * $p<0.05$ and ** $p<0.01$ from vehicle; + $p < 0.05$ from vehicle plus breast cancer cells or conditioned medium; $ $p<0.05$ from vehicle and RANKL treated cultures.

Fig. 5. PTN induces osteoclast apoptosis. (A) *In vitro* survival of mature osteoclasts after withdrawal of human RANKL (100ng/ml), M-CSF (25ng/ml), or both followed by exposure to MDA-231-BT1 conditioned medium (20%v/v) in the presence or absence of PTN for 24 hours. (B-C) *In vitro* caspase-3/7 activation (B) DNA fragmentation (C) in mature osteoclasts from the experiment described in panel A after 6 and 24 hours, respectively. (D) *In vitro* osteoclast apoptosis in cultures treated with PTN (10μM) in the presence of absence of the caspase inhibitor zVAD-fmk (20μM). Values are mean ± SD; * $p<0.05$ and ** $p<0.01$ from vehicle; $ $p<0.05$ from vehicle plus breast cancer conditioned medium; + $p < 0.05$ from PTN plus caspase inhibitor zVAD-fmk.

Fig. 6. PTN inhibits skeletal tumour growth and reduces breast cancer-induced osteolysis. (A) Graphic representation of supracalvarial injection of conditioned medium (CM) from human MDA-231-BT1 and MCF7 and mouse 4T1-BT1 breast cancer cells in immunocompetent mice pretreated with vehicle or PTN (3mg/kg/day) for 3 days. (B) Total bone volume from the experiment described in panel A (n = 7). (C) Graphic representation of intra-tibial injection of the mouse breast cancer osteotropic 4T1-BT1 in immunocompetent BALB/c mice pretreated with vehicle (DMSO/water: 0.1:10) or PTN (10mg/kg/day) for 12 days. (D) Total bone volume (BV/TV), trabecular thickness (Tb.Th.) and connectedness density (Conn.D) in tibial metaphysis of mice from the experiment described in panel C. (E) Tumour size from the experiment described in panels C-D. (F) *In vivo* osteoclast formation (Oc.N, left panel) and activity (Oc.S/BS, right panel) from the

experiment described in panels C-D. (G) *In vivo* osteoblast number (Ob.N, left panel), osteoid surface (Ob.S/BS, middle panel) and osteoid width (Ob.W, right panel) from the experiment described in panels C-F. Values are mean ± SD; * $p<0.05$ and ** $p<0.01$ from vehicle plus breast cancer cells or conditioned medium.

Figure 1

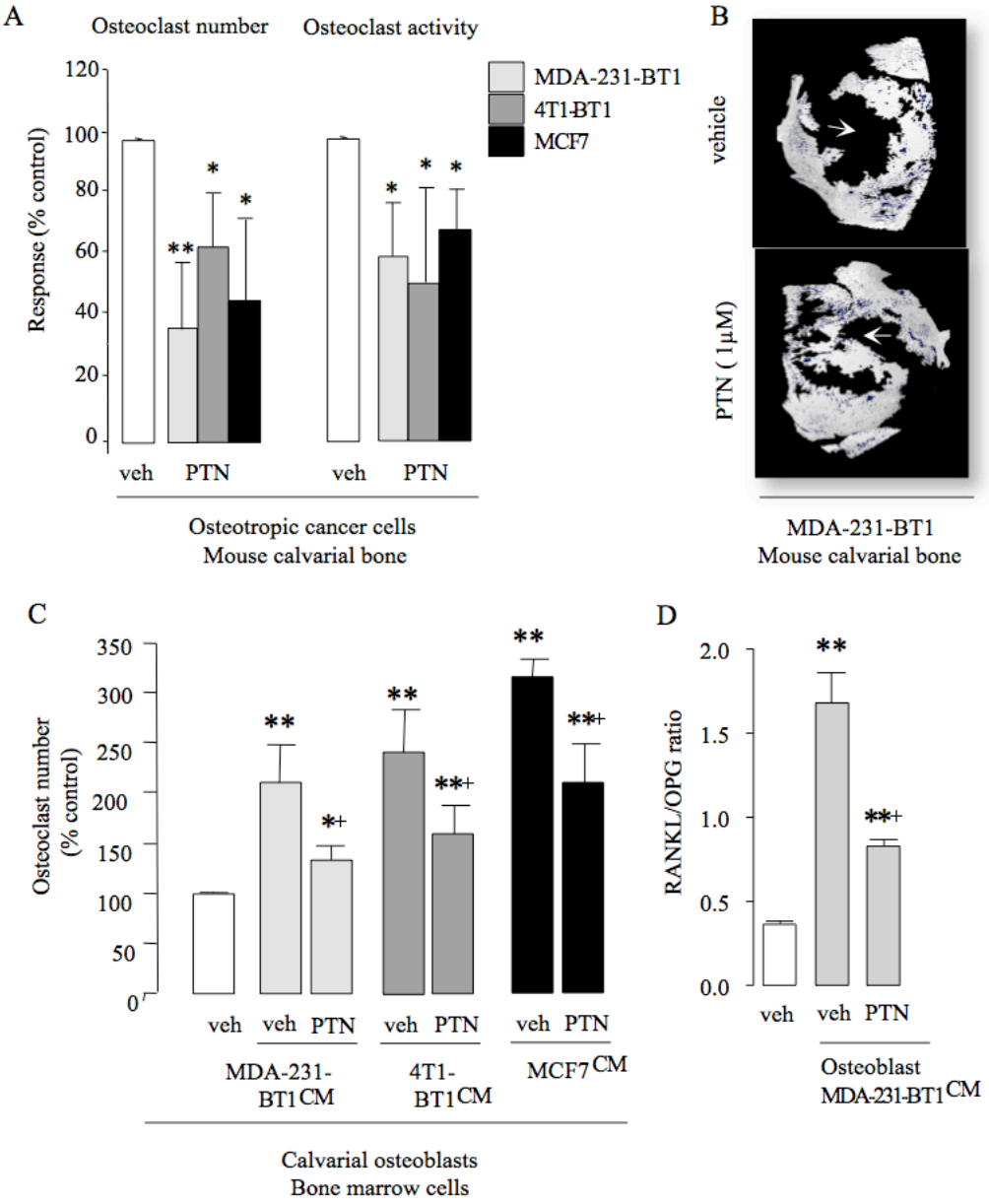
A
Osteoclast number
Osteoclast activity
MDA-231-BT1
4T1-BT1
MCF7
Response (% control)
120
100
80
60
40
20
0
veh
PTN
veh
PTN
Osteotropic cancer cells
Mouse calvarial bone
B
vehicle
PTN (1μM)
MDA-231-BT1
Mouse calvarial bone
C
Osteoclast number
(% control)
350
300
250
200
150
100
50
0
veh
veh
PTN
veh
PTN
veh
PTN
MDA-231-BT1 CM
4T1-BT1 CM
MCF7 CM
Calvarial osteoblasts
Bone marrow cells
D
RANKL/OPG ratio
2.0
1.5
1.0
0.5
0.0
veh
veh
PTN
Osteoblast
MDA-231-BT1 CM

Figure 2

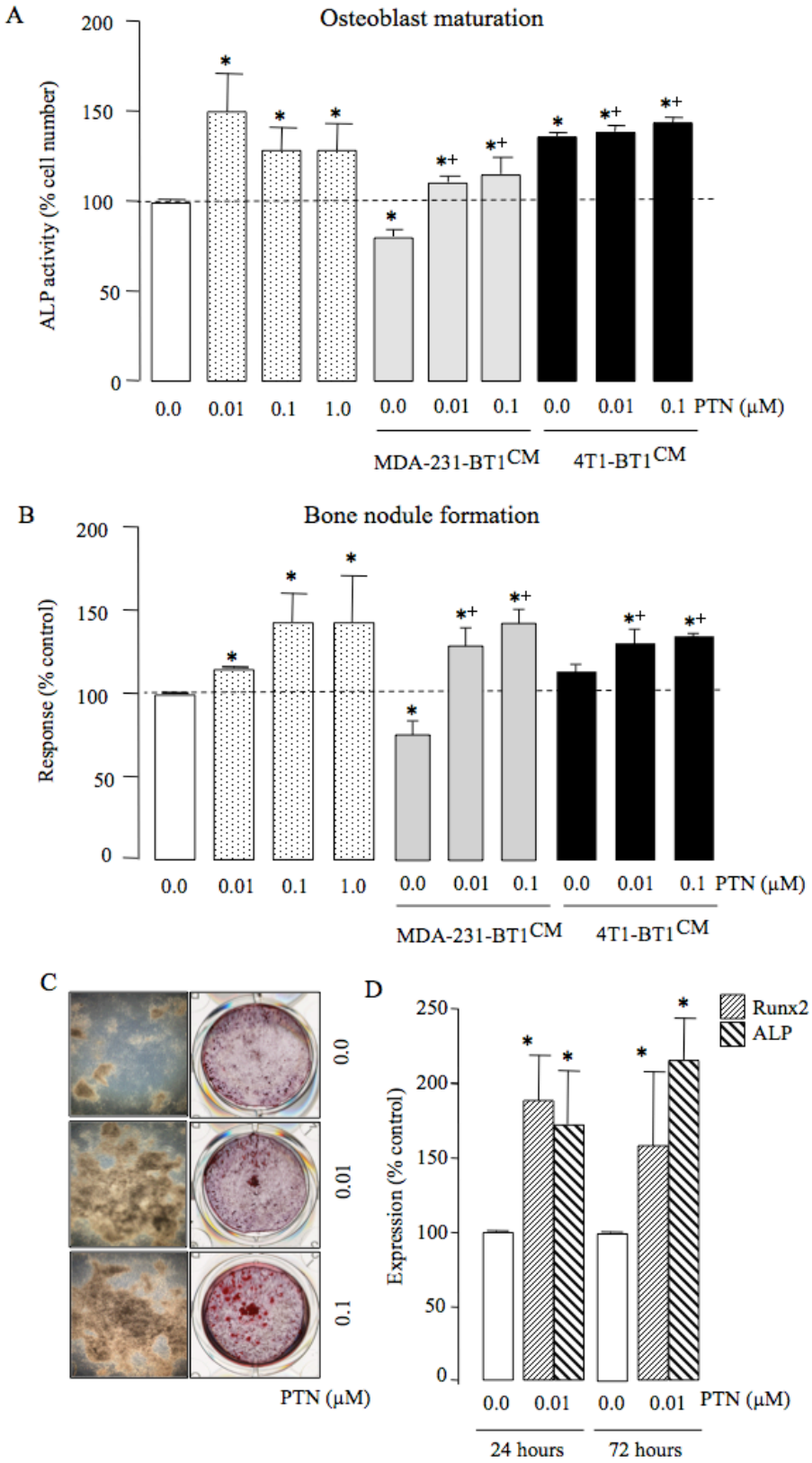
A
Osteoblast maturation
ALP activity (% cell number)
200
150
100
50
0
0.0
0.01
0.1
1.0
0.0
0.01
0.1
0.0
0.01
0.1
PTN (μM)
MDA-231-BT1CM
4T1-BT1CM
B
Bone nodule formation
Response (% control)
200
150
100
50
0
0.0
0.01
0.1
1.0
0.0
0.01
0.1
0.0
0.01
0.1
PTN (μM)
MDA-231-BT1CM
4T1-BT1CM
C
0.0
0.01
0.1
PTN (μM)
D
Runx2
ALP
Expression (% control)
250
200
150
100
50
0
0.0
0.01
0.0
0.01
PTN (μM)
24 hours
72 hours

Figure 4

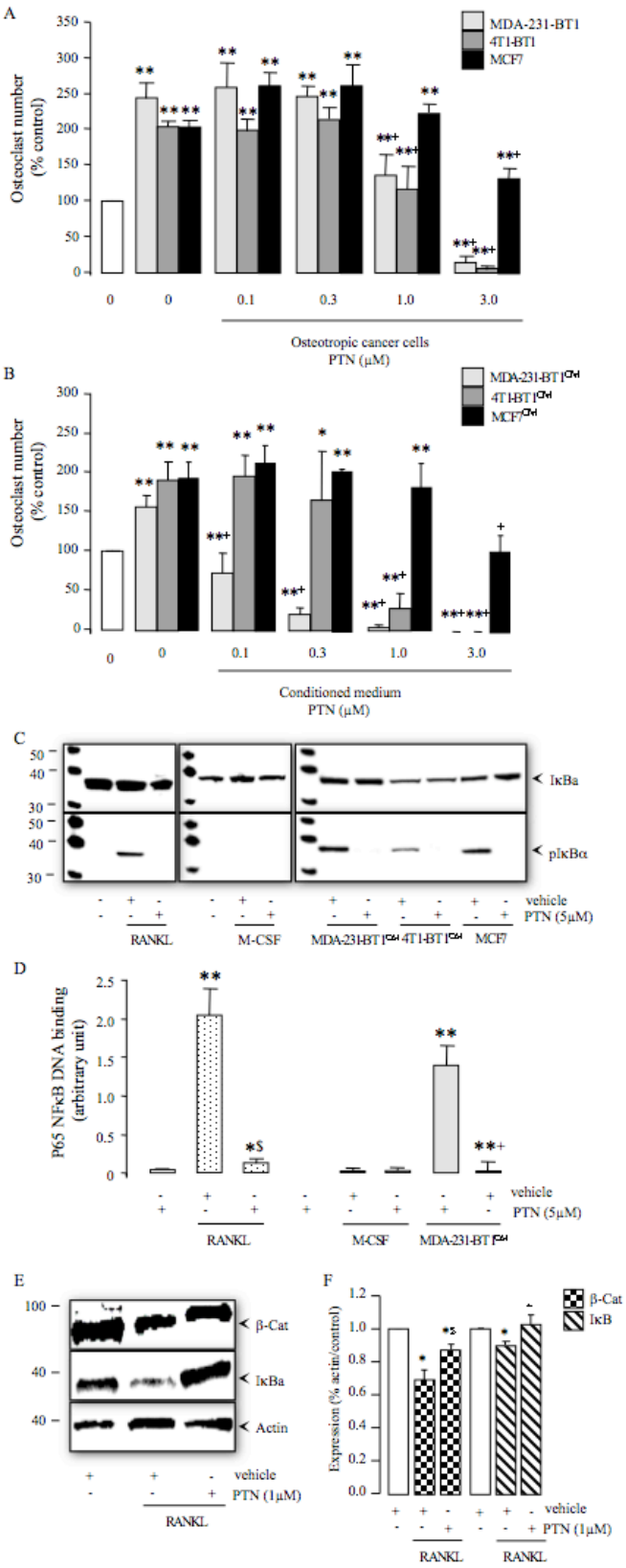
A
Osteoclast number (% control)
MDA-231-BT1
4T1-BT1
MCF7
Osteotropic cancer cells
PTN (μM)
B
Osteoclast number (% control)
Conditioned medium
PTN (μM)
C
IκBa
pIκBα
vehicle
PTN (5μM)
RANKL
M-CSF
D
P65 NFκB DNA binding (arbitrary unit)
vehicle
PTN (5μM)
RANKL
M-CSF
E
β-Cat
IκBa
Actin
vehicle
PTN (1μM)
RANKL
F
Expression (% actin/control)
β-Cat
IκB
vehicle
PTN (1μM)
RANKL
RANKL

Figure 3

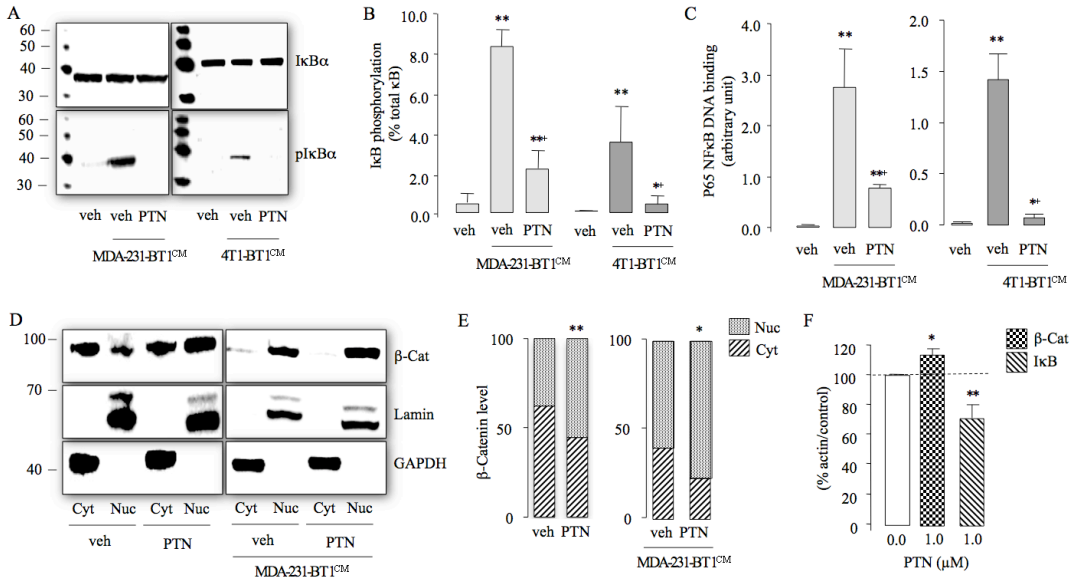
A
60
50
40
30
IκBα
pIκBα
veh veh PTN veh veh PTN
MDA-231-BT1CM
4T1-BT1CM
B
IκB phosphorylation (% total κB)
10.0
8.0
6.0
4.0
2.0
0.0
veh veh PTN veh veh PTN
MDA-231-BT1CM
4T1-BT1CM
C
P65 NFκB DNA binding (arbitrary unit)
4.0
3.0
2.0
1.0
0.0
2.0
1.5
1.0
0.5
0.0
veh veh PTN veh veh PTN
MDA-231-BT1CM
4T1-BT1CM
D
100
70
40
β-Cat
Lamin
GAPDH
Cyt Nuc Cyt Nuc Cyt Nuc Cyt Nuc
veh PTN veh PTN
MDA-231-BT1CM
E
β-Catenin level
100
50
0
Nuc
Cyt
veh PTN
MDA-231-BT1CM
F
β-Cat
IκB
(% actin/control)
120
100
80
60
40
20
0
0.0 1.0 1.0
PTN (μM)

Figure 6

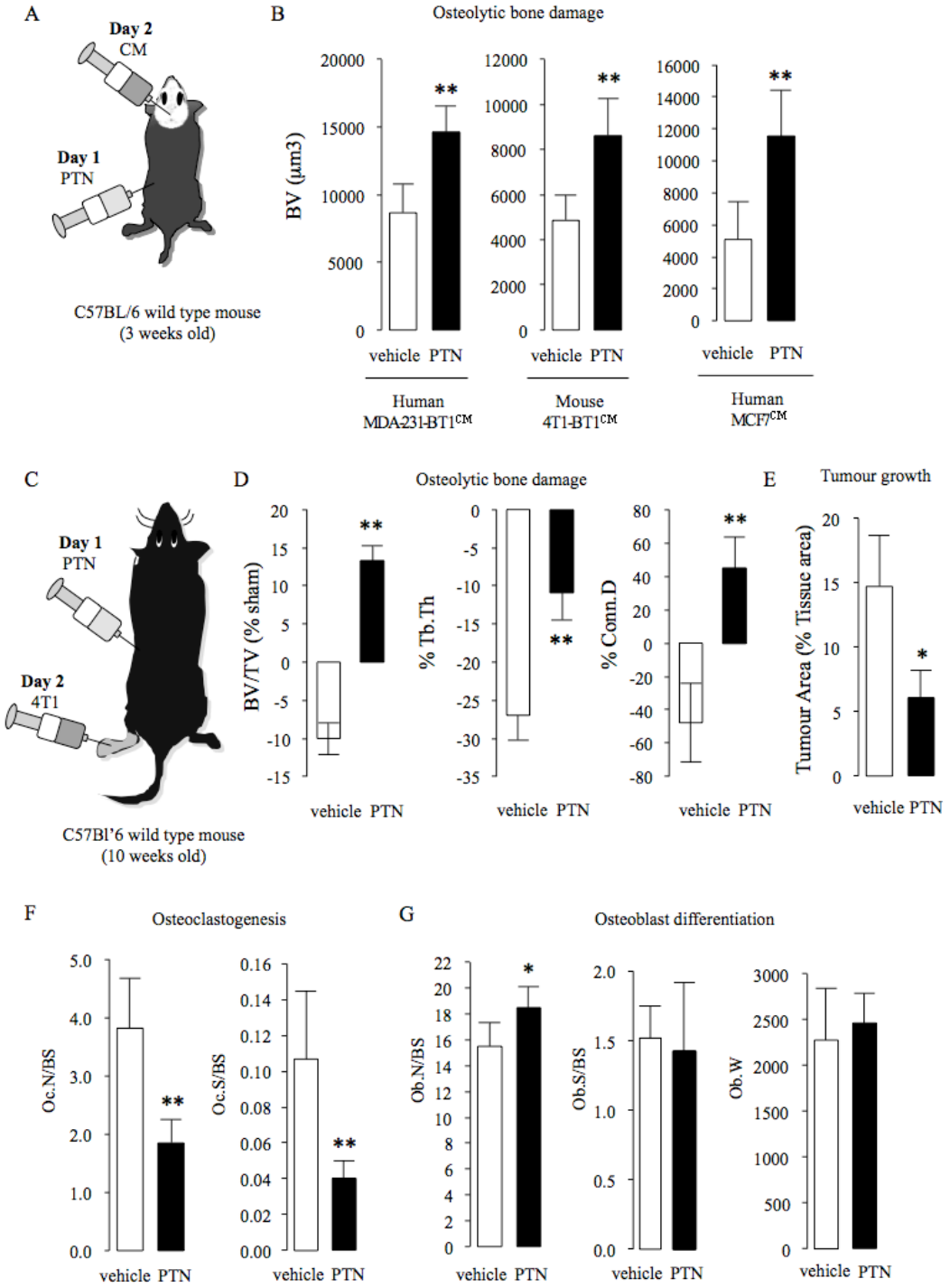
A
Day 2
CM
Day 1
PTN
C57BL/6 wild type mouse
(3 weeks old)
B
Osteolytic bone damage
BV (µm3)
vehicle PTN
Human
MDA-231-BT1CM
Mouse
4T1-BT1CM
Human
MCF7CM
C
Day 1
PTN
Day 2
4T1
C57Bl'6 wild type mouse
(10 weeks old)
D
Osteolytic bone damage
BV/TV (% sham)
% Tb.Th
% Conn.D
E
Tumour growth
Tumour Area (% Tissue area)
F
Osteoclastogenesis
Oc.N/BS
Oc.S/BS
G
Osteoblast differentiation
Ob.N/BS
Ob.S/BS
Ob.W

Figure 5

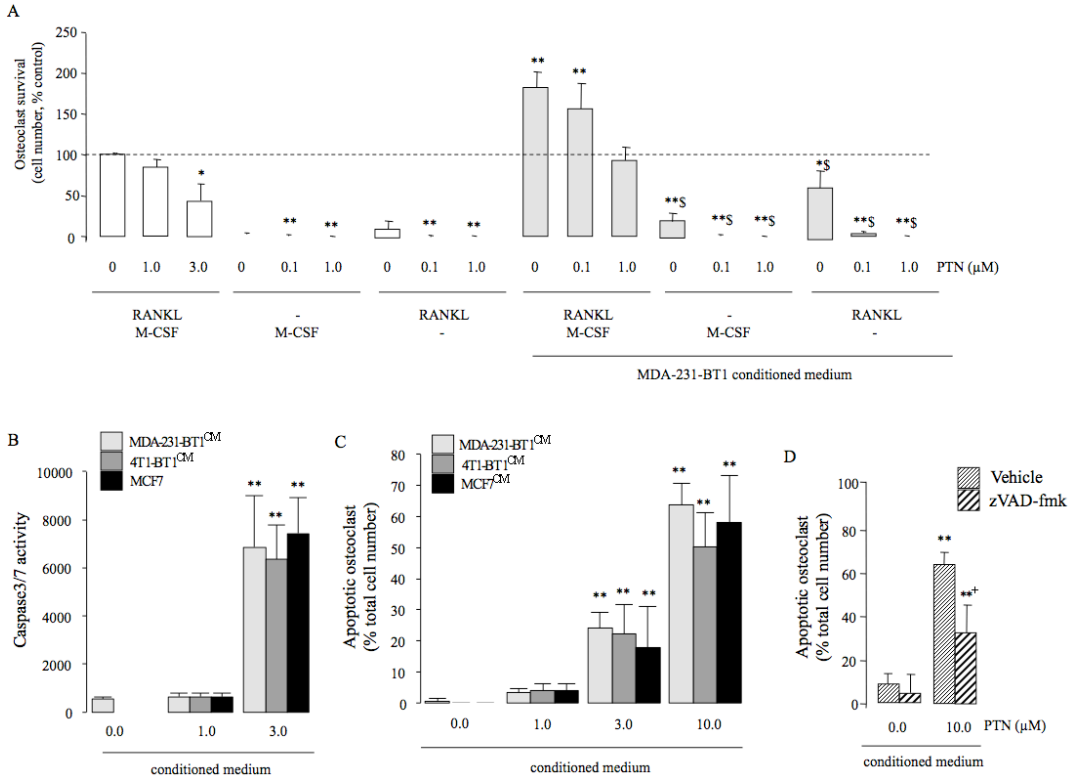
A
Osteoclast survival (cell number, % control)
250
200
150
100
50
0
0 1.0 3.0 0 0.1 1.0 0 0.1 1.0 0 0.1 1.0 0 0.1 1.0 0 0.1 1.0 PTN (μM)
RANKL M-CSF
- M-CSF
RANKL -
RANKL M-CSF
- M-CSF
RANKL -
MDA-231-BT1 conditioned medium
B
MDA-231-BT1CM
4T1-BT1CM
MCF7
Caspase3/7 activity
10000
8000
6000
4000
2000
0
0.0 1.0 3.0
conditioned medium
C
MDA-231-BT1CM
4T1-BT1CM
MCF7CM
Apoptotic osteoclast (% total cell number)
80
70
60
50
40
30
20
10
0
0.0 1.0 3.0 10.0
conditioned medium
D
Vehicle
zVAD-fmk
Apoptotic osteoclast (% total cell number)
100
80
60
40
20
0
0.0 10.0 PTN (μM)
conditioned medium

Supplemental figures

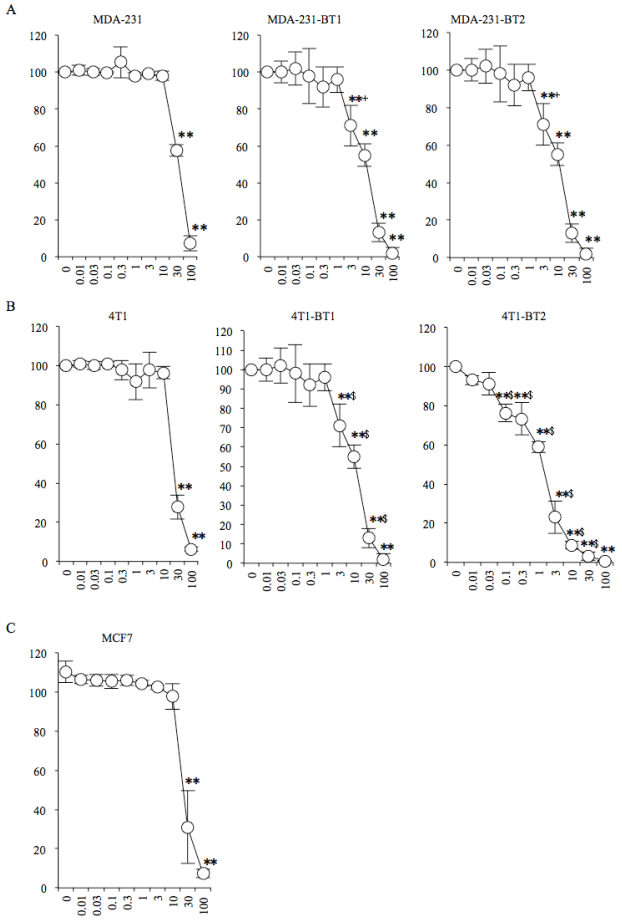

Figure S1. Effects of Parthenolide on the growth of osteotropic breast cancer cells *in vitro* (related to Table 1). (A) *In vitro* growth of human parental (left, MDA-231) and osteotropic (middle, MDA-231-BT1; right, MDA-231-BT2) breast cancer cells treated with vehicle (DMSO, 0.01%v/v) or PTN at the indicated concentrations for 48 hours. (B) *In vitro* growth of mouse parental (left, 4T1) and osteotropic (middle, 4T1-BT1; right, 4T1-BT2) breast cancer cells treated with vehicle (DMSO, 0.01%v/v) or PTN at the indicated concentrations for 48 hours. (C) *In vitro* growth of human MCF7 breast cancer cells treated with vehicle (DMSO, 0.01%v/v) or PTN at the indicated concentrations for 48 hours. Cell growth was measured after 48 h of continuous exposure to PTN by AlamarBlue assay. BT denotes osteotropic. Values are mean ± SD; ** $p < 0.01$ from vehicle treated cultures, + $p<0.01$ from correspondent concentration in parental MDA-231 cultures; $ $p<0.01$ from correspondent concentration in parental 4T1 cultures.

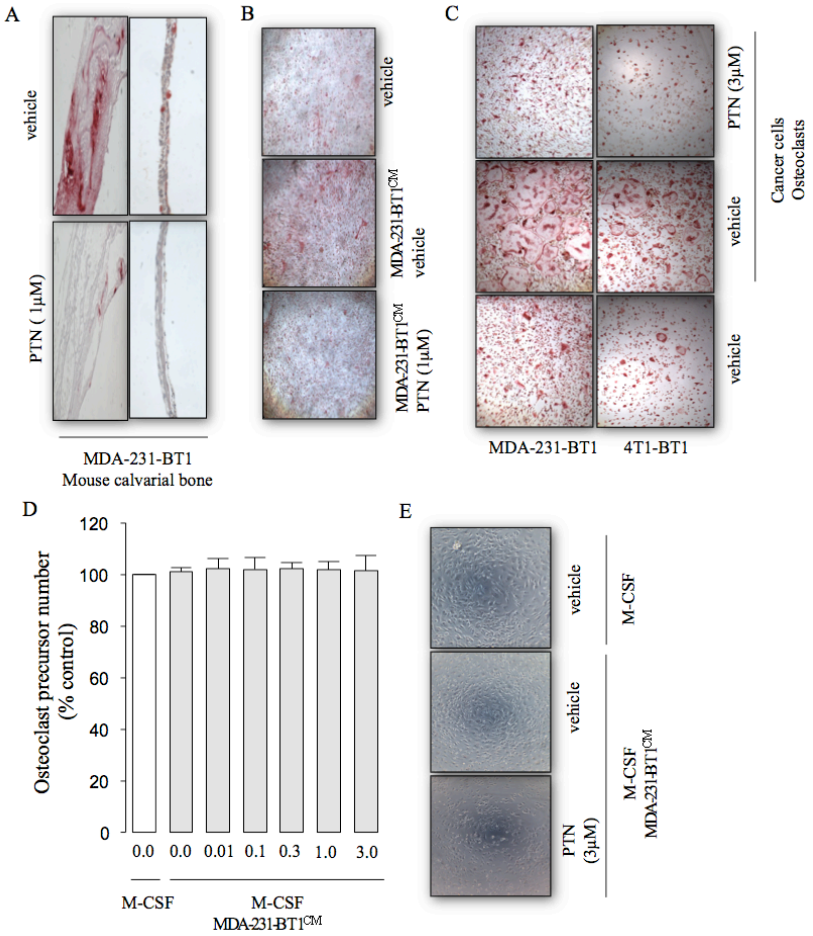

Figure S2. Effects of PTN on osteoclast formation and activity *in vitro*. (A) Representative photomicrographs of osteoclasts from the experiment described in Fig. 1A (left panel). (B) Representative photomicrographs of osteoclasts from the experiment described in Fig. 1C. (C) Representative photomicrographs of osteoclasts from the experiment described in Fig. 4B. (D) *In vitro* proliferation of pre-osteoclast cells in mouse bone marrow cultured with M-CSF (25 ng/ml) and conditioned medium (20% v/v) from human MDA-231 breast cancer cells treated with vehicle (0.1% DMSO) or Parthenolide (PTN) at the indicated concentrations for 48 hours. (E) Representative photomicrographs of M-CSF (25ng/ml) generated bone marrow cells from the experiment described in panel D.

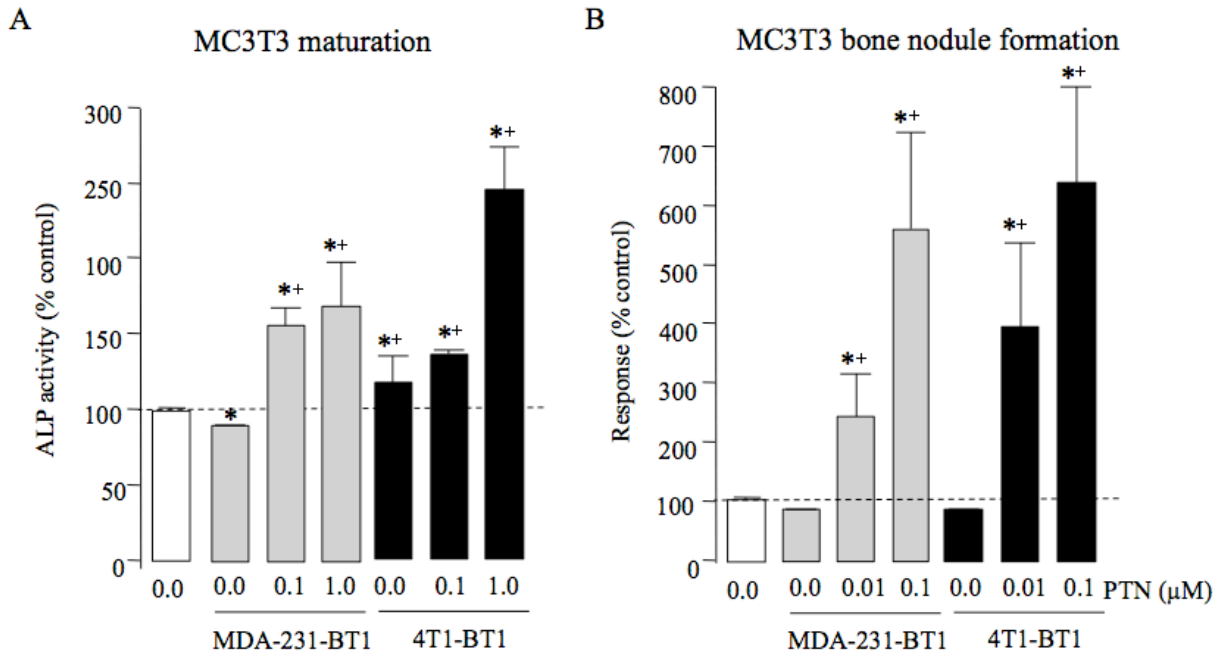

Figure S3. PTN enhances MC3T3 differentiation and bone nodule formation. (A-B) *In vitro* osteoblast differentiation (A) and bone nodule formation (B) in cultures of mouse osteoblast-like cells MC3T3 exposed to standard or conditioned medium (20%v/v) from human MDA-231-BT1 or mouse 4T1-BT1 cancer cells in the presence or absence of PTN for 7 days. Osteoblast differentiation and bone nodule formation were assessed by Alkaline phosphatase (ALP) and Alazarin Red assays. Values are mean ± SD; * $p<0.05$ from vehicle; + $p<0.05$ from vehicle plus breast cancer cell conditioned medium.

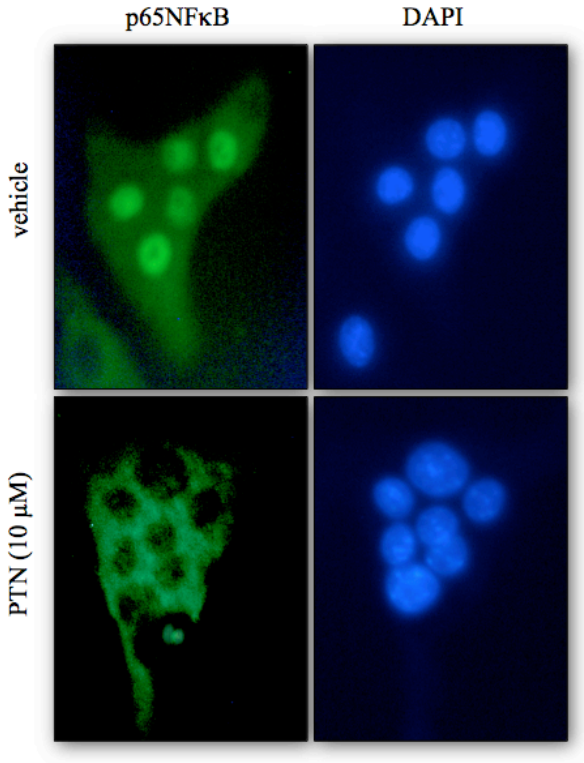

Figure S4. Effect of PTN on RANKL-induced NFκB nuclear translocation in osteoclasts. M-CSF and RANKL-generated osteoclasts were cultured in serum-free medium in the presence of vehicle or Parthenolide (PTN, 10μM) for 1 hour before stimulation with RANKL (100ng/ml) for 25 minutes. Osteoclasts were stained for p65 NFκB (green) and nuclei counterstained with DAPI (blue) as described under materials and methods.

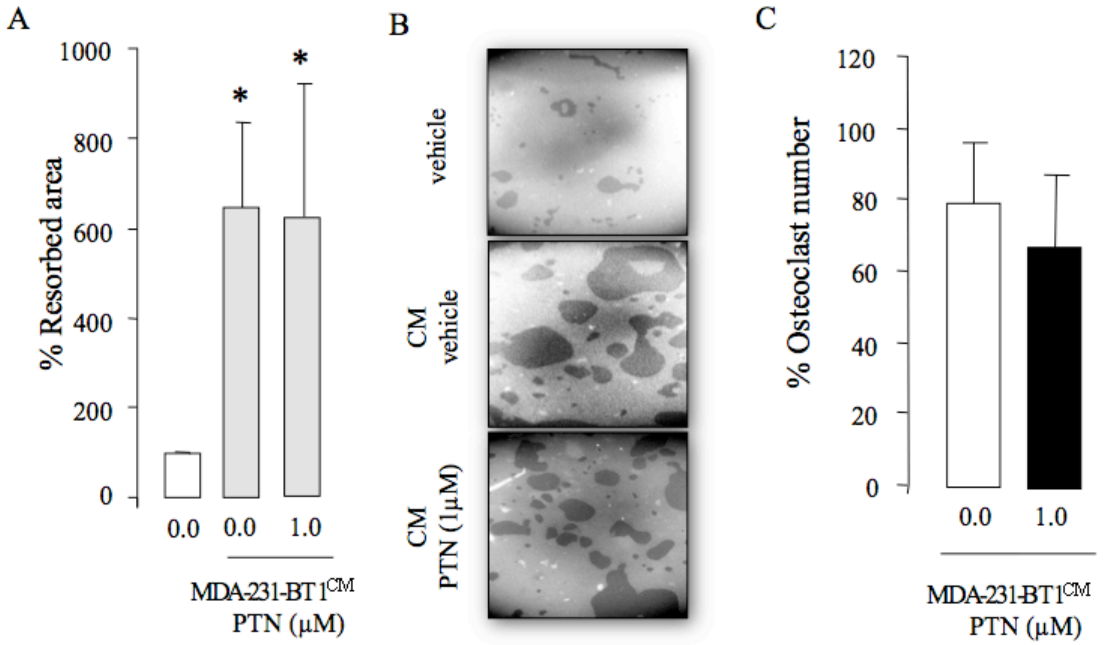

Figure S5. Effects of Parthenolide on osteoclast bone resorption *in vitro*. (A) *In vitro* bone resorption in mature osteoclast cultures after exposure to human MDA-231 conditioned medium (20% v/v) in the presence and absence of PTN (1μM) after 72 hours. (B) Representative photomicrographs of resorbed areas from the experiment described in panel A. (C) Total osteoclast number from the experiment described in panels A-B. Values are mean ± SD; * $p<0.05$ from vehicle treated cultures.

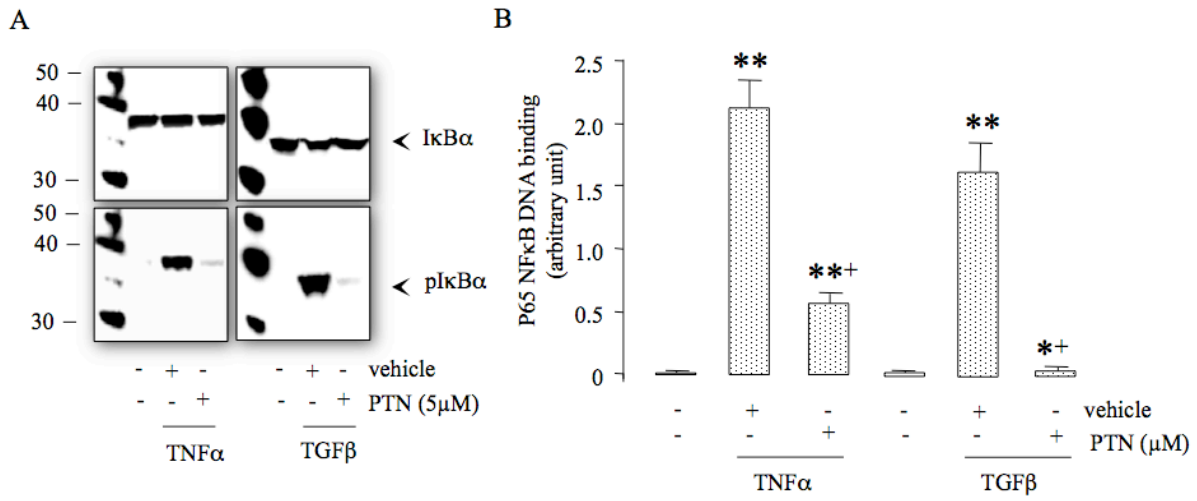

Figure S6. Effects of Parthenolide TNFα– and TGFβ-induced NFκB activation. Western blot of (A) total and phosphorylated IκB and (B) quantification of p65 NFκB – DNA binding in M-CSF (25ng/ml) dependent pre-osteoclasts cultured in MDA-231-BT1 conditioned medium and vehicle (0.01%DMSO) or Parthenolide (PTN, 5μM) for 1 hour and then exposed to human TNFα (10ng/ml) or human TGFβ (10ng/ml) for 10 (A) or 45 minutes (B). Values are mean ± SD; ** $p<0.01$ from vehicle treated cultures; + $p<0.01$ from vehicle, cytokine and breast cancer cells or conditioned medium treated cultures.

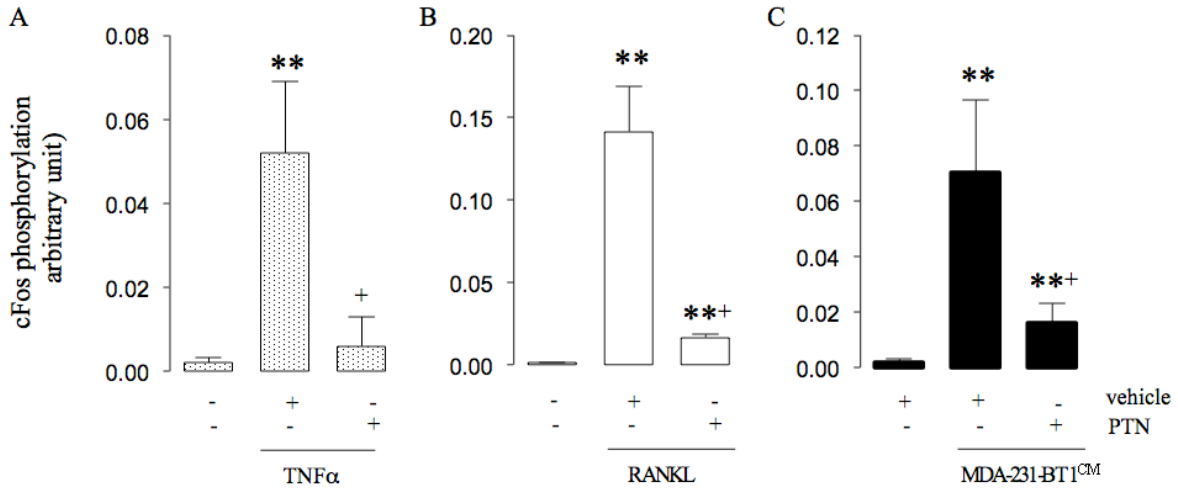

Figure S7. Parthenolide inhibits cFos signaling in pre-osteoclasts. Phosphorylation of cFos in M-CSF dependent pre-osteoclasts exposed to TNFα (A, 10ng/ml), RANKL (B, 100ng/ml) or human MDA-231 conditioned medium (C, 20%v/v) in the presence and absence of Parthenolide (PTN, 5μM). Values are mean ± SD; ** $p < 0.01$ from vehicle treated cultures; + $p<0.01$ from vehicle and cytokine or breast cancer cells or conditioned medium treated cultures.